VNU Journal of Science: Mathematics – Physics, Vol. 34, No. 1 (2018) 8-13

VNU Journal of Science: Mathematics - Physics

Journal homepage: https://js.vnu.edu.vn/MaP

Blue, Green and Yellow Emissions at the Same Time from Mn-doped ZnS Microbelts

Nguyen Van Nghia[1,2,*], Nguyen Duy Hung[1]

[1]*Advanced Institute of Science and Technology (AIST), Hanoi University of Science and Technology (HUST), 01 Dai Co Viet, Hanoi, Vietnam*

[2]*Thuy Loi University, 175 Tay Son, Dong Da, Hanoi, Vietnam*

Received 23 July 2017
Revised 22 September 2017; Accepted 27 September 2017

Abstract: An investigation of the morphology, structure, composition and optical properties of ZnS:Mn^{2+} microbelts grown by the thermal evaporation method using ZnS powder and $MnCl_2.4H_2O$ powder as precursor materials is presented. The SEM images of the products show that ZnS:Mn^{2+} microbelts are bigger and shorter than ZnS microbelts. EDS reveals that the composition of the microbelts include Zn, S, O, Mn and Cl elements. The atom rate of oxygen composition of the doped microbelts seems to be slightly lower than undoped ones. XRD pattern of the prepared microbelts shows that ZnO coexists with ZnS on the undoped microbelts. However, at the Mn-doped microbelts, the component phase of ZnO is disappeared. Photoluminescence spectra of undoped ZnS microbelts reveal a strong broad emission band at visible wavelength region and a weak ultraviolet band. Interestingly, when Mn^{2+} is doped into the microbelts, the visible emission band is separated into blue, green, and yellow bands peaking at around 442, 520 nm, and 572 nm, respectively. The effects of Mn^{2+} ions on the emission bands are discussed in detail.

Keywords: ZnS :Mn^{2+} microbelts, photoluminescence, thermal evaporation.

1. Introduction

ZnS, an II–VI semiconductor, has been extensively investigated due to its potential applications in optics, photoelectronics, sensors, catalysts and so on [1–3]. Recently, numerous efforts have been employed to control the fabrication of micro and nanomaterials with various morphologies, since the novel properties and potential applications of nanomaterials depend sensitively on their shapes and sizes [4]. Because of doping ZnS with different metal ions, novel characteristics, such as stable and

* Corresponding author. Tel.: 84-984915472.
Email: nghiaaist@gmail.com

https//doi.org/ 10.25073/2588-1124/vnumap.4212

tunable optical properties, could be obtained [5–7]. Among them, Mn-doped ZnS nanocrystals have been receiving much attention due to their promising application in optoelectronic devices [8]. A large number of Mn-doped ZnS nanocrystals with simple morphologies, such as thin film, nanowires, and nanorods have been prepared by various techniques [9–11]. The most reports of Mn-doped ZnS focused on the emission due to $^4T_1 \rightarrow {}^6A_1$ transition within the 3d shell of Mn^{2+}. Usually, Mn-doped ZnS structures have two emission bands, one yellow-orange band of Mn^{2+} and the other of ZnS host material. In our work, we synthesize Mn-doped ZnS microbelts by thermal evaporation and report on their photoluminescence properties with three different peaks in visible region to demonstrate that the Mn concentration plays an important role in tuning the emission of radiative centers in ZnS microbelts.

2. Experiment

The undoped and Mn-doped ZnS microbelts were synthesized on silica substrates by thermal vapor deposition in a conventional horizontal quartz tube furnace. ZnS powder and a mixing of high-purity ZnS and $MnCl_2.4H_2O$ powders as the precursor materials were placed into an alumina boat and positioned at the center zone of the horizontal tube furnace. Silica substrates with size of 0.5 x 0.5 cm were placed in the low temperature zone at about 20 cm downstream from the aluminum boat. A haft of the quartz tube containing the aluminum boat and silica substrates was setup outside the tube furnace until the furnace was heated to deposition temperature. The quartz tube was pumped down to pressure of 1×10^{-3} Torr and heated to 300 ^oC, then the high-purity argon was introduced into the tube and the mechanical rotary pump was turn off. The flow rates of Ar were controlled by a mass flow meter at 160 sccm. The temperature of the furnace was raised continually to growth temperature at a ramping rate of 10 ^oC/min. The deposition temperature was set up at 1100 ^oC. When temperature of the furnace increased to 900 ^oC, the part of quartz tube containing the aluminum boat and silica substrates was pushed into the furnace to grow microbelts. During synthesis the furnace temperature was maintained at growth temperature for 30 min, after that the furnace was allowed to cool naturally to room temperature.

3. Results and discussion

In order to study the morphology of the structures, FESEM were employed. Fig. 1 shows a series of FESEM images of the microstructures grown on silica substrates. A typical FESEM image shows that undoped ZnS microbelts are high density with several hundred nanometers to about one micron in widths and tens of microns in lengths (Fig. 1a). These microbelts are quite smooth and randomly oriented. For Mn-doped ZnS, the microstructures turned into bigger and shorter microbelts. Furthermore, the density of the microbelts seems to be reduced and the surface of them is rough with some black dots in it. The corresponding EDS spectra reveal that the undoped microbelts mainly contain Zn, S and O elements and the atom ratio of undoped ZnS is 47.5, 36.5 and 16.0 at%. The origin of O atom may come from reaction between ZnS and O_2 which exist in the furnace tube and are not pumped to low enough pressure. For Mn^{2+} doped microbelts, the atom ratio of oxygen reduces a little to around 15.4 %. Also, the Cl and Mn components appear with atom ratios of about 10.6 % and 1.6 % respectively for the doped products. The Cl composition can exist on the microbelts due to reaction between Zn and Cl to form $ZnCl_2$.

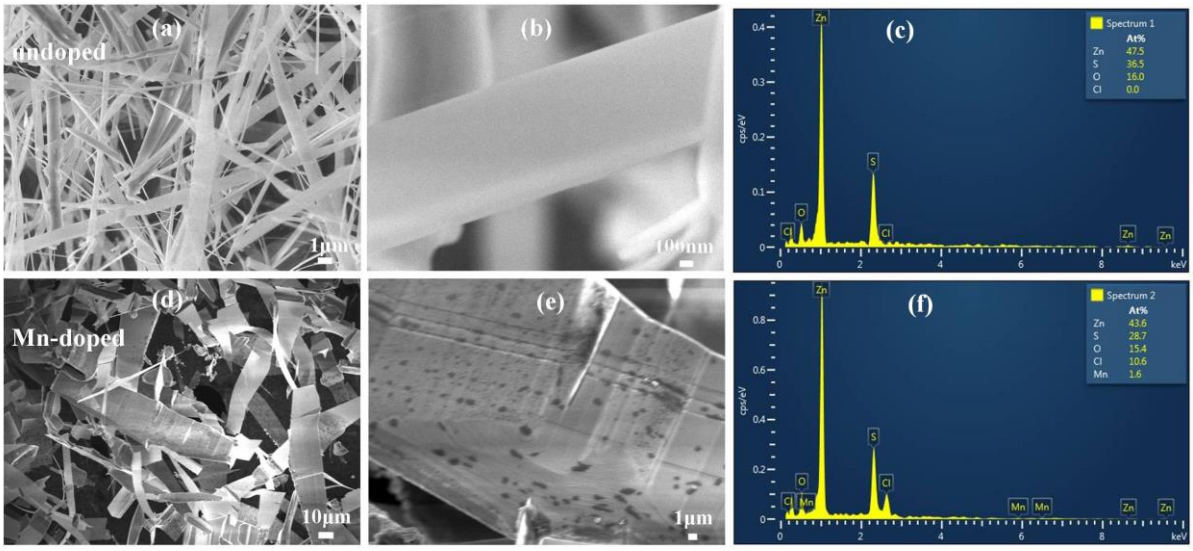

Figure 1. FESEM images with low and high magnification and EDS of undoped ZnS microbelts (a,b,c), and Mn-doped ZnS microbelts (d,e,f).

Furthermore, XRD measurement was performed in order to determine the crystalline phase of the microstructures. It is clear from Figure 2 that all of microbelts doped or undoped Mn are matched to the structure of wurtzite (JCPDS 05-0492). In detail, the XRD pattern of the undoped microbelts shows the ZnO peaks beside the main phase of ZnS. The phase of ZnO is matched to the structure of wurtzite (JCPDS no.36-1451). The XRD pattern of undoped sample matched well with EDS analysis above, in which, there are Zn, S, and O elements at the same time. However, at Mn-doped ZnS microbelts, only ZnS phase is detected and no phase related to Mn or Cl being observed in XRD patterns. The reason of that may be due to the concentration of Mn or Cl in the microbelts is too small and XRD measurements cannot recognize the presence of them in the microbelts. The phase of ZnO disappeared in XRD pattern of these microbelts may be due to Mn prevented O from combining with Zn and S elements.

To investigate the optical propertie of the structures, the PL spectra of undoped and Mn-doped ZnS microbelts were measured at room temperature using a 275-nm excitation wavelength as shown in Fig. 3. From this figure, for the undoped sample, PL spectrum shows two emission bands at ultraviolet and visible regions. The ultraviolet band is due to band to band transition of ZnS, ZnO or ZnOS [12, 13]. The blue band peaking at 493 nm may be associated with point defects such as the isolated Zn vacancies in the single negative charge states or other oxygen-related centers of self-activated or interstitial sulphur impurities [1, 14, 15]. However, in the visible emission band, the doped Mn microbelts show three peaks, at 442 nm (blue), 520 nm (green), and 572 nm (yellow). Morever, the UV emission band has a trend to be quenched. The blue emission band at around 442 nm is attributed to the surface defects such as sulfur vacancy or sulfur interstitial lattice defects [2, 3, 5]. Meanwhile, the green emission at around 520 nm may be assigned to the surface defects such as oxygen vacancies [16]. The yellow emission at around 572 nm is associated with the $^4T_1$–$^6A_1$ transition within the 3d shell layer of Mn^{2+} [18,19, 20].

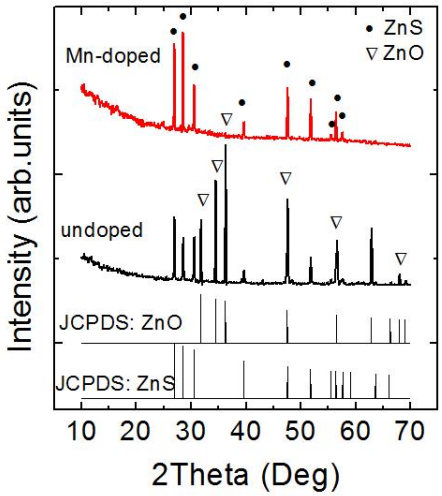

Figure 2. XRD pattern of ZnS and Mn-doped ZnS microbelts grown on silica substrates.

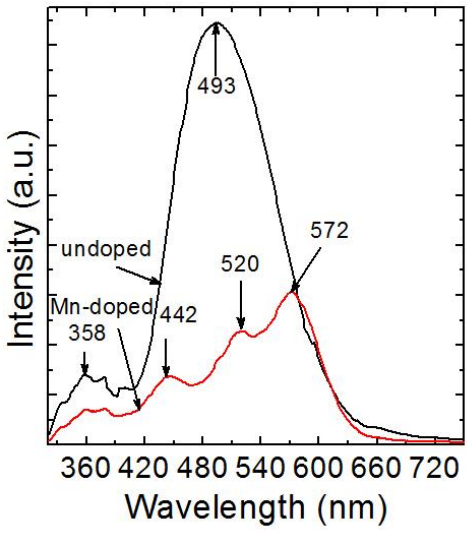

Figure 3. PL spectra of undoped and Mn-doped ZnS microbelts.

Furthermore, the effect of Mn on the radiative centers of ZnS microbelts are investigated by analysing the PLE spectra shown in Figure 4. In fact, excitation pathway for the emission of Mn^{2+} in the microbelts has two ways, namely the energy transfers directly from the ZnS host and another from the radiative defects to the 3d states of Mn^{2+} [7]. The PLE measurements monitored at the emission wavelength of 570 nm. At undoped sample, the spectra show that the microbelts are absorbed strongly at about 345 nm to 376 nm which are corresponded with the bandgap of ZnS, ZnO or ZnOS [12], [21]. However, at the Mn-doped ZnS microbelts, there is a PLE peak at around 337 nm corresponding to

band gap of ZnS (3.686 eV). The absorption edge was shifted to short wavelength, it means that the absorption related to the band to band transition of ZnO or ZnOS reduces when Mn is doped in ZnS host. These results show that Mn^{2+} modified the emission of the radiative centers of ZnS microbelts.

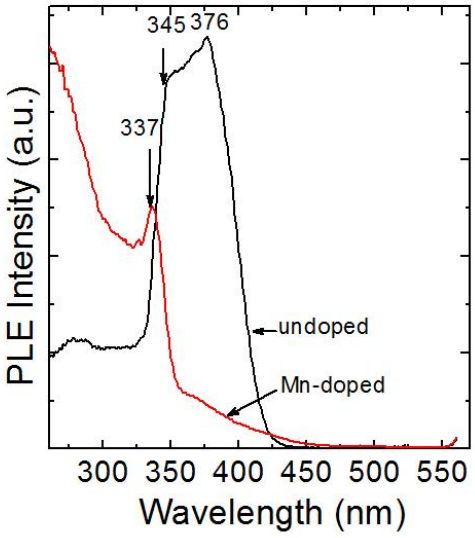

Figure 4. PLE spectra of undoped and Mn-doped ZnS microbelts.

4. Conclusion

The undoped and Mn doped ZnS microbelts on silica substrates have been successfully prepared by a thermal evaporation method. The undoped ZnS microbelts show a broad band emission at visible region around 493nm which related to radiative centers of ZnS and ZnO. By doping Mn, the emission band of radiative centers related to S and O in the ZnS microbelts separated into blue, green, and yellow emissions. The UV emission band has a trend to be quenched at the Mn-doped sample. Therefore, the emission of radiative centers of ZnS can be controlled by Mn doped into ZnS microbelts.

References

[1] G. H. Yue et al., Hydrothermal synthesis of single-crystal ZnS nanowires, Appl. Phys. A Mater. Sci. Process., vol. 84, no. 4, (2006) 409.

[2] A. Goudarzi et al., Low-Temperature Growth of Nanocrystalline Mn-Doped ZnS Thin Films Prepared by Chemical Bath Deposition and Optical Properties, Chem. Mater., vol. 21, no. 12, (2009) 2375.

[3] W. W. G. Becker and A. A. J. Bard, Photoluminescence and photoinduced oxygen adsorption of colloidal zinc sulfide dispersions, J. Phys. Chem., vol. 78712, no. 24, (1983) 4888.

[4] T. T. Q. Hoa et al., Optical properties of Mn-doped ZnS semiconductor nanoclusters synthesized by a hydrothermal process, Opt. Mater. (Amst)., vol. 33, no. 3, (2011) 308.

[5] S. Wageh, Z. S. Ling, and X. Xu-Rong, Growth and optical properties of colloidal ZnS nanoparticles, J. Cryst. Growth, vol. 255, no. 3–4, (2003) 332.

[6] K. Sooklal, B. S. Cullum, S. M. Angel, and C. J. Murphy, Photophysical Properties of ZnS Nanoclusters with Spatially Localized Mn 2+, J. Phys. Chem., vol. 100, no. 11, (1996) 4551.

[7] S. Sapra, A. Prakash, A. Ghangrekar, N. Periasamy, and D. D. Sarma, Emission properties of manganese-doped ZnS nanocrystals, J. Phys. Chem. B, vol. 109, no. 5, (2005) 1663.

[8] B. J. Ge, J. Wang, H. Zhang, X. Wang, Q. Peng, and Y. Li, Halide-Transport Chemical Vapor Deposition of Luminescent ZnS : Mn 2 + One-Dimensional Nanostructures, no. 2, (2005) 303.

[9] B. Y. Geng et al., Synthesis and photoluminescence properties of ZnMnS nanobelts, vol. 2157, (2004) 10.

[10] X. J. Hao, A. P. Podhorodecki, Y. S. Shen, G. Zatryb, J. Misiewicz, and M. A. Green, Effects of Si-rich oxide layer stoichiometry on the structural and optical properties of Si QD / SiO_2 multilayer films, Nanotechnology, vol. 20, no. 48, (2009) 485703.

[11] W. Tang and D. C. Cameron, Electroluminescent zinc sulphide devices produced by sol-gel processing, Thin Solid Films, vol. 280, no. 1–2, (1996) 221.

[12] D. Q. Trung, N. Tu, N. D. Hung, and P. T. Huy, Probing the origin of green emission in 1D ZnS nanostructures, J. Lumin., vol. 169, (2016) 165.

[13] N. Kumbhojkar, V. V. Nikesh, A. Kshirsagar, and S. Mahamuni, Photophysical properties of ZnS nanoclusters, J. Appl. Phys., vol. 88, no. 11, (2000) 6260.

[14] John S. McCloy and Barrett G. Potter, Photoluminescence in Chemical Vapor Deposited ZnS: insight into electronic defects, OPTICAL MATERIALS EXPRESS, Vol. 3, No. 9, (2013) 1273.

[15] Ji-Hong Zhao, Chun-Hao Li, Jun-Jie Xu, Ya-Wei Hao, and Xian-Bin Li, Surface modification of nanostructured ZnS by femtosecond laser pulsing, Applied Surface Science 293 (2014) 332.

[16] H. Tang, B. J. Kwon, J. Kim, and J. Y. Park, Growth modes of ZnS nanostructures on the different substrates, J. Phys. Chem. C, vol. 114, no. 49, (2010) 21366.

[17] T. Mitsui, N. Yamamoto, T. Tadokoro, and S. Ohta, Cathodoluminescence image of defects and luminescence centers in ZnS/GaAs (100), J. Appl. Phys., vol. 80, no. 12, (1996) 6972.

[18] R. N. Bhargava, D. Gallagher, X. Hong, and A. Nurmikko, Optical Properties of Manganese-Doped of ZnS," Phys. Rev. Lett., vol. 72, no. 3, (1994) 1.

[19] Jitao Li, Kuili Liu, Xinying Zhu, Ming Meng, Wei Qin, Quantao Liu, and Chunxiang Xu, Competitive mechanism of electron transition in Mn-doped ZnS nanoribbons, Journal of Alloys and Compounds 658 (2016) 616.

[20] H.J. Yuan, X.Q. Yan, Z.X. Zhang, D.F. Liu, Z.P. Zhou, L. Cao, J.X. Wang,Y. Gao, L. Song, L.F. Liu, X.W. Zhao, X.Y. Dou, W.Y. Zhou, and S.S. Xie, Synthesis, optical, andmagnetic properties of $Zn_{1-x}Mn_xS$ nanowires grown by thermal evaporation, Journal of Crystal Growth 271 (2004) 403.

[21] Ngo Xuan Dai, Do Thanh Long, Nguyen Ngoc Long, and Nguyen Thi Thuc Hien, Fabrication and Photoluminescence Properties of ZnS Nanoribbons and Nanowires, Journal of the Korean Physical Society, vol. 52, no. 5, (2008) 1530.